Chapter 6

EVOKED COMPOUND ACTION POTENTIAL WIDTHS

The contents of this chapter is included in an article entitled:
Smit, J. E., Hanekom, T. and Hanekom, J. J. (2008) Estimation of stimulus attenuation in cochlear implants, *submitted for publication*

6.1 INTRODUCTION

The Type I ANF model described in Chapter 5 has to be verified against experimentally measured temporal characteristic data. This chapter and the next (Chapter 7) focus on applications of the ANF model to *a*) verify the model; and *b*) determine the model's applicability as part of larger models to address questions pertaining to the cochlear implant research field.

Most of the earlier temporal characteristic measurement studies centred on observations from single-fibres in cats and guinea-pigs, while more recent studies increasingly make use of gross ensemble observations through ECAP measurements. ECAP profile width data can be used to examine the extent to which psychophysical measurements reflect the amount of neural excitation spread (Cohen *et al.*, 2003; Miller *et al.*, 2003). The development of a comprehensive model to simulate ECAPs is beyond the scope of this study. However, ECAP profile widths can be used to estimate stimulus at-

tenuation. Stimulus attenuation (characterized by length constant) directly relates to current distribution and thus the extent of neural excitation inside the cochlea (Black and Clark, 1980; Spelman, Clopton and Pfingst, 1982; Black *et al.*, 1983; Kral *et al.*, 1998; Vanpoucke, Zarowski and Peeters, 2004).

This chapter focuses on the influence of the variation in the stimulus attenuation on neural excitation spread for monopolar stimulation of an electrode located in the basal part of the cochlea. The Type I ANF model was used to predict the width of neural excitation as a result of specific stimuli. The objective of this chapter is to develop a simple method to estimate stimulus attenuation values by calculating the values of stimulus attenuation that best fit the modelled excitation profile widths to the measured ECAP profile widths.

6.2 MODEL AND METHODS

6.2.1 Models of the implanted cochlea and auditory nerve fibre

Simulations were performed using the resistances from a 3D spiralling finite element volume-conduction model of the first one-and-a-half turns of the electrically stimulated human cochlea, coupled to the human ANF model (Figures 6.1(a) and (b)). The amplitudes of stimulation pulses at the nerve fibres were derived from the external potential distribution, which was in turn calculated from the Ohmic resistances from the volume-conduction model. Simulations were performed with two versions of the ANF model, simulating the effects of non-degenerate and degenerate nerve fibres respectively.

The modelled cochlea was stimulated with a monopolar electrode configuration, with the stimulated electrode located in the basal cochlear turn and the return electrode lying outside the cochlea. The pulsatile stimulus waveform was a biphasic, charge-balanced, square pulse without interphase gap, with equal cathodic and anodic phases of 40 μs duration. Only single-pulse responses were calculated.

Simulations were performed for two electrode array positions, one lateral (Nucleus 24

straight array) and one medial (Nucleus contour array), relative to the modiolus (Cohen *et al.*, 2003; Miller *et al.*, 2004). The straight array was modelled with full-band electrodes and the contour array with half-band electrodes (Miller *et al.*, 2004).

6.2.2 ECAP profile widths at the electrode array level

The output of the ANF model is a neural excitation profile (Figures 6.1(c) and 6.2), at the location of the ANFs (subsequently called neural level), showing the stimulus intensity at which a nerve fibre at a specific location along the length of the basilar membrane will be excited. To compare the predicted excitation widths and NRT results, the excitation widths, i.e. the ECAP profile widths, at the location of the stimulating electrode array (subsequently called electrode array level) need to be determined. Ideally, this will be done by solving the inverse problem, referred to as the "backward problem" (for details see Briaire and Frijns, 2005).

To facilitate estimation of the stimulus attenuation factor, a simple approximation to solving the inverse problem is used. The data of Cohen *et al.* (2003) provide ECAP response widths at various loudness levels, specified as percentages of the MCL. The position of the modelled probe electrode corresponded to Cohen *et al.*'s (2003) electrode 6 (i.e. a basal position). To model ECAP profile widths, the measured dynamic range data for electrode 6 of each of the seven Cohen *et al.* (2003) subjects were mapped onto the estimated neural excitation profiles. Mapping was performed by translating the dynamic range data to decibel values above threshold (defined at zero decibel) corresponding to the 20, 50 and 80% loudness levels for each subject. The estimated widths of the ECAP response at the neural level at these loudness levels were then read from the modelled neural excitation profiles (Figures 6.1(c) and 6.2).

A dimensionless, normalised potential step (value = 1 for activated nerve fibres, and zero elsewhere) was generated for each of these widths (Figure 6.1(d)) and used as the source in the calculation of potential field distributions at the electrode array level (Figure 6.1(e)). To perform these calculations, three simplifications with regard to real cochleae were made. Firstly, an isotropic medium was assumed in the space between the neural and electrode array levels, although an anisotropic medium was assumed in the volume-conduction cochlear model. Secondly, constant distances were assumed between the neural level and each of the respective electrode array levels.

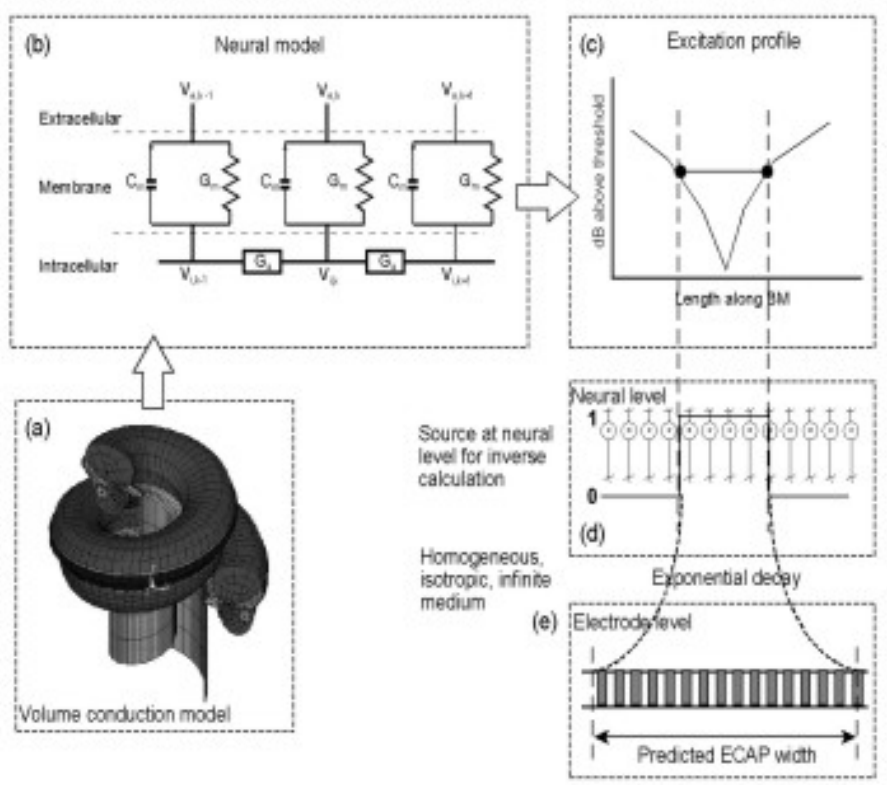

Figure 6.1: Outline of the simple method used to estimate ECAP profile widths at the electrode array level for non-degenerate and degenerate nerve fibres. Representations of the (a) volume-conductance cochlear model and (b) nerve fibre model. (c) The output of the ANF model is a neural excitation profile indicating the threshold currents at which the nerve fibres along the basilar membrane become excited. (d) Neural excitation spread is estimated at the neural level and e) the simple method estimates ECAP profile widths at the electrode array level.

Values for these distances were sourced from the volume-conduction model. Thirdly, a transverse exponential decay of voltage inside the scala tympani was assumed (Black and Clark, 1980; O'Leary, Black and Clark, 1985). Using an estimated value for the stimulus attenuation, each potential field distribution at the electrode array level was derived as the summation of the potential field contributions of all the activated ANFs as specified by the individual step functions. The full width half maximum (FWHM) of each distribution, i.e. the width of the potential distribution at 50% of its peak amplitude, determined the excitation widths, similar to the technique used by Cohen *et al.* (2003).

6.3 RESULTS

6.3.1 Neural excitation profiles

Neural excitation profiles were calculated with the ANF model (Figures 6.2(a) and (b)). For contour array stimulation profiles for degenerate nerve fibres predicted wider profiles, compared to straight array stimulation where the non-degenerate and degenerate nerve fibre populations predicted similar profile widths. Neural excitation profile widths were determined as discussed in Section 6.2.2.

Neural excitation profiles widths were also calculated with the GSEF model by Frijns and ten Kate (1994) and Frijns *et al.* (1995; 2000) in combination with the same volume-conduction model used in this study (Figures 6.2(c) and (d)). For details refer to Hanekom (2001b).

GSEF model neural excitation profiles differed from those of the ANF model. In contrast to the ANF model the GSEF model predicted similar neural excitation profiles, and hence profile widths, for degenerate and non-degenerate nerve fibre populations when stimulated with the contour array. For the straight array wider neural excitation profiles are predicted for a degenerate than a non-degenerate nerve fibre population.

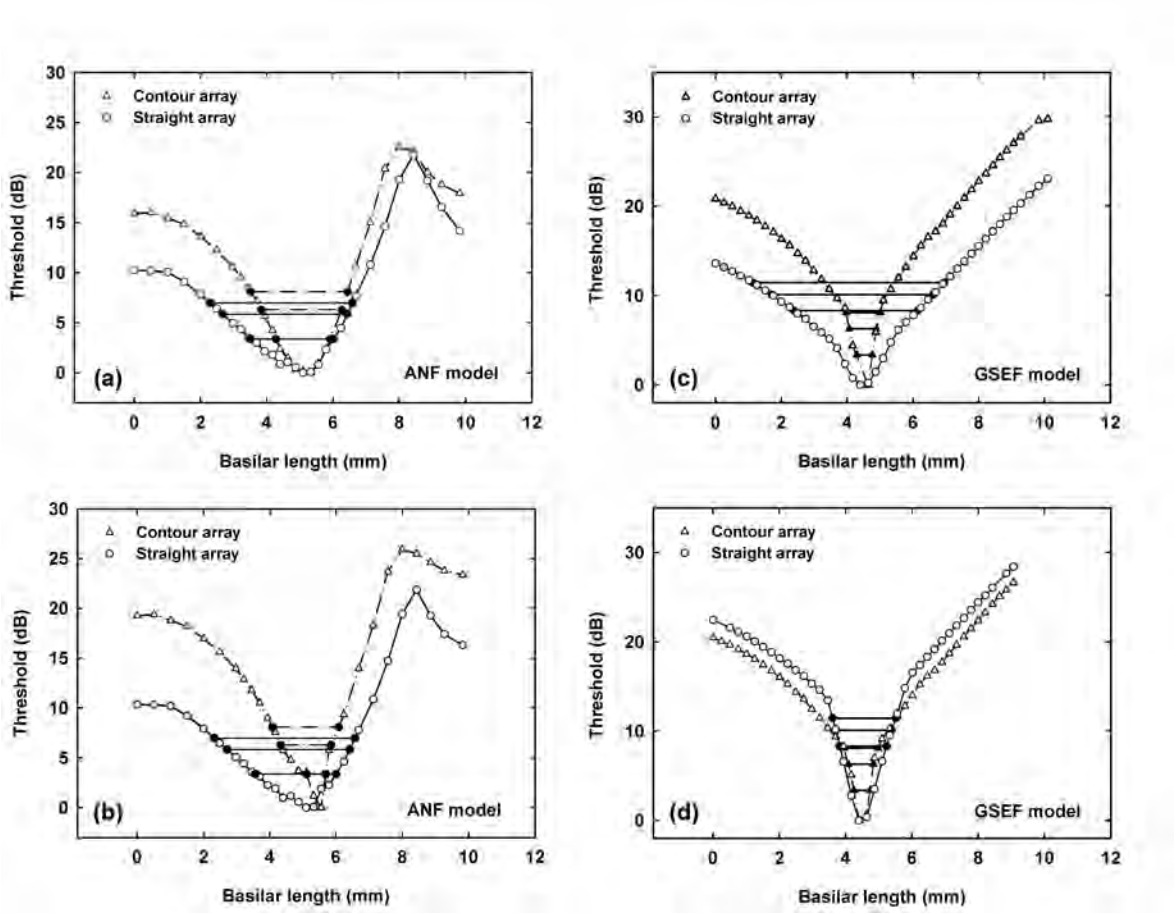

Figure 6.2: (a, b) Neural excitation profiles calculated with the volume-conduction-ANF model (open markers). Predicted neural excitation profile widths for 20, 50 and 80% loudness levels for Cohen *et al.*'s (2003) subjects S3 (straight array, solid lines) and C1 (contour array, dot-dash lines) for (a) a degenerate and (b) a non-degenerate ANF population are indicated with horizontal lines. (c, d) Neural excitation profiles simulated with the GSEF model combined with the volume-conduction model. All conditions are the same as in (a) and (b).

Table 6.1: Measured ECAP profile width ranges for electrode 6 (Cohen *et al.*, 2003) for four straight array and three contour array subjects. Width data at the 20% level were available for only one subject using the straight array, and for none of the subjects using the contour array. Profile widths were measured at FWHM, i.e. the profile width at 50% of the peak amplitude.

	80% loudness level	**50% loudness level**	**20% loudness level**
Straight array	4.26 mm to 6.78 mm	4.58 mm to 6.67 mm	3.73 mm (measured for single subject)
Contour array	2.98 mm to 3.41 mm	2.13 mm to 3.62 mm	No data available

6.3.2 Predicted versus measured ECAP profile widths

6.3.2.1 Measured ECAP profile widths

Cohen *et al.* (2003) reported the widths of the ECAP profiles at FWHM at 20, 50 and 80% loudness levels. The width ranges of seven subjects, four straight array and three contour array subjects, for probe electrode 6 are summarised in Table 6.1.

Width data at the 20% level were available for only one subject using the straight array, and for none of the subjects using the contour array. Cohen *et al.* (2003) observed that the profile widths of the contour array are narrower than those of the straight array.

6.3.2.2 Auditory nerve fibre model predicted ECAP profile widths

Predicted ECAP profile width results at the electrode array level for degenerate and non-degenerate ANF populations respectively, are shown in Table 6.2. A stimulus attenuation of 5.5 dB/mm was used in the simulations for goodness of fit to the Cohen *et al.* (2003) results. This value was within the range of stimulus attenuation values reported in literature (Black and Clark, 1980; Black *et al.*, 1983; Kral *et al.*, 1998) and was arrived at after consideration of the results presented in Table 6.3 and Figure 6.3(a) and (b). The width of the distribution was taken at FWHM.

The ECAP profile widths for both the straight and contour arrays followed the expected trend, i.e. to decrease with a decrease in loudness level. However, if the profile

Table 6.2: Simulated ECAP profile widths at the electrode array level for a stimulation attenuation of 5.5 dB/mm. Similar to Cohen *et al.* (2003) profile widths were measured at FWHM, i.e. the profile width at 50% of the peak amplitude.

	80% loudness level	**50% loudness level**	**20% loudness level**
Straight array: degenerate	3.88 mm to 6.76 mm	3.88 mm to 5.86 mm	3.65 mm to 5.29 mm
Contour array: degenerate	3.67 mm to 3.82 mm	3.31 mm to 3.67 mm	3.15 mm
Straight array: non-degenerate	3.48 mm to 6.64 mm	3.48 mm to 5.39 mm	2.92 mm to 5.09 mm
Contour array: non-degenerate	3.44 mm to 3.57 mm	3.21 mm to 3.44 mm	3.02 mm

width ranges between the two arrays were compared, the difference in width at the electrode array level was smaller compared to the difference observed at the neural level. The contour array also demonstrated narrower profile width ranges than the straight array. Furthermore, the profile width values for the contour array lay closer to the lower limit of the value range for the straight array.

Comparison between the degenerate and non-degenerate cases for the straight array predicted similar width ranges, with the degenerate case slightly wider than the non-degenerate case. For the contour array the width ranges for the degenerate case were wider than for the non-degenerate case. The reason for these differences is that at the neural level, the neural excitation profiles for the degenerate and non-degenerate cases were similar, while for the contour array there was a marked difference between the two cases.

6.3.2.3 Normalised ECAP profile width ranges

Figures 6.3(a) and (b) shows the simulated ECAP profile width ranges calculated with the ANF model, normalised to the width ranges measured by Cohen *et al.* (2003). Normalisation was done by dividing measured values by predicted widths. The ECAP profile widths for the straight array generally compared well for both degenerate and non-degenerate ANF cases, with the measured ranges at the 80% level reasonably centred on the predicted ranges, although the upper limits were underestimated by up to 48%. For the 50% levels the width ranges were underestimated, but were within

53% of the upper limits of the measured ranges. Cohen *et al.* (2003) measured the ECAP profile width for only one straight array subject at the 20% level, and the predicted value overestimated the measured valued by about 30%.

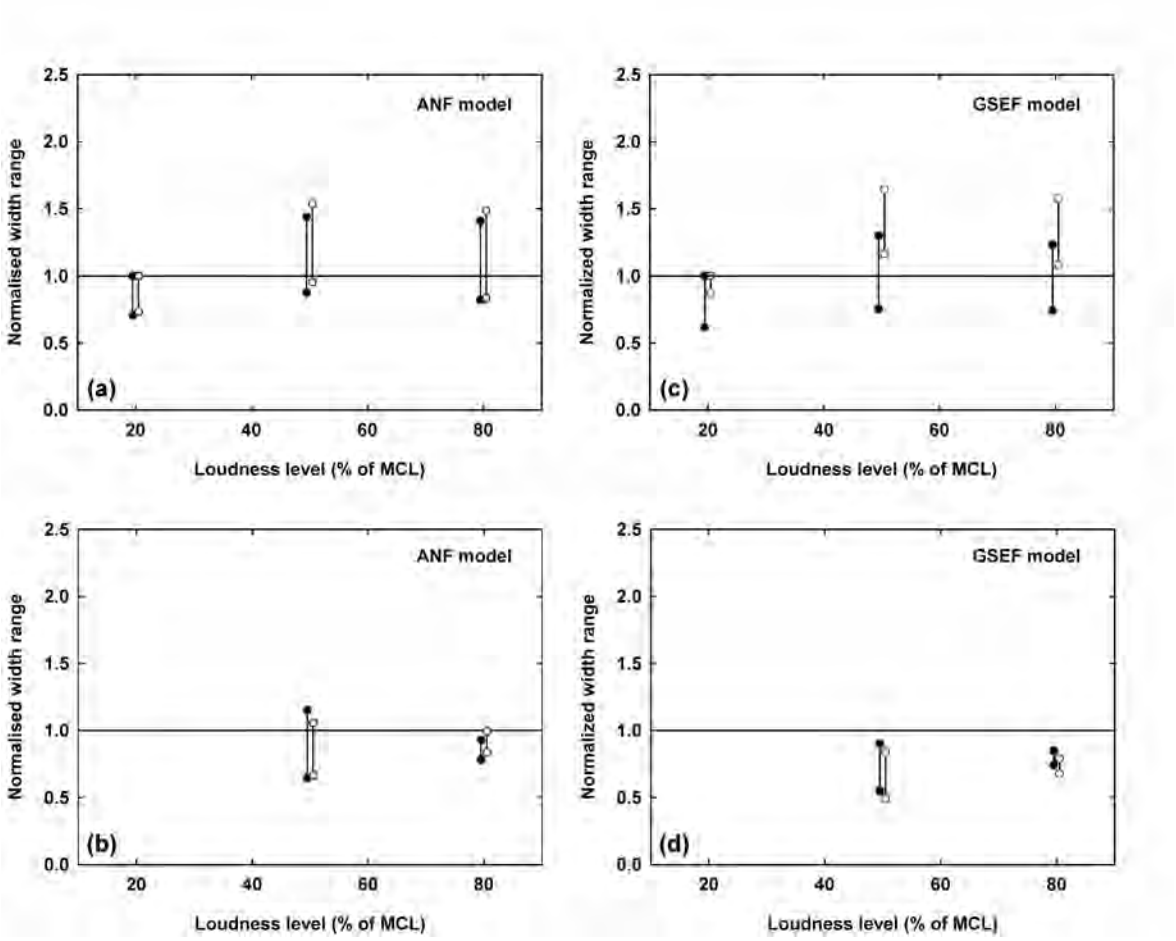

Figure 6.3: Normalised ECAP profile width ranges, at the electrode array level, calculated with the ANF model for 20, 50 and 80% loudness levels for (a) straight array and (b) contour array for a degenerate and non-degenerate ANF population. Calculations are for a stimulus attenuation of 5.5 dB/mm. Filled symbols indicates degenerate and open symbols non-degenerate ANF cases respectively. The horizontal line indicates the predicted widths. (c, d) Normalised ECAP profile width ranges calculated with the GSEF model. ECAP profile widths shown are for a stimulus attenuation of 3.5 dB/mm. All conditions are the same as in (a) and (b).

Width ranges at the 80% level were overestimated for the contour array, but the upper limits of the measured ranges were within 22% of the predicted ranges. The upper limits of the measured values at the 50% level were overestimated up to 36%

by the predicted values, while the lower limits fell within 15% underestimation by the predicted values.

Normalised ECAP width ranges calculate with the GSEF model for straight and contour arrays for degenerate and non-degenerate nerve fibre populations are shown in Figures 6.3(c) and (d). Normalisation was done in the same way as for Figures 6.3(a) and (b). The best fit to the Cohen *et al.* (2003) results was for a stimulus attenuation of 3.5 dB/mm. The contour array demonstrated narrower profile width ranges than the straight array. The profile width ranges between the two arrays for the non-degenerate case were also similar, in contrast to the larger differences observed for the degenerate case (compare with Figures 6.2(c) and (d)). Furthermore, the profile width values for the contour array lie closer to the upper limit of the value range for the straight array. The reasons for these differences lay in the way the two cases were modelled, with resultant similar potential step functions for the non-degenerate case resulting in similar neural response potential distributions.

6.3.3 Stimulus attenuation predicted with the auditory nerve fibre model

To exemplify the effect of stimulus attenuation on ECAP profile widths, the latter (for Cohen's subject S3) are shown as a function of stimulus attenuation at the electrode array level (Figure 6.4). Results for the other subjects were similar and are not shown. The ECAP profile widths decreased with increasing stimulus attenuation and asymptotically approached zero for large values of the stimulus attenuation.

The stimulus attenuation values that provided the best fit to Cohen *et al.*'s (2003) results are presented in Table 6.3. Owing to lack of information about the 20% loudness level data for the contour array, no stimulus attenuation values could be estimated. It appeared as though i) stimulus attenuation was relatively unchanged between the 50 and 80% loudness levels but increased for the 20% level and ii) that intersubject variation in stimulus attenuation existed at a specific loudness level.

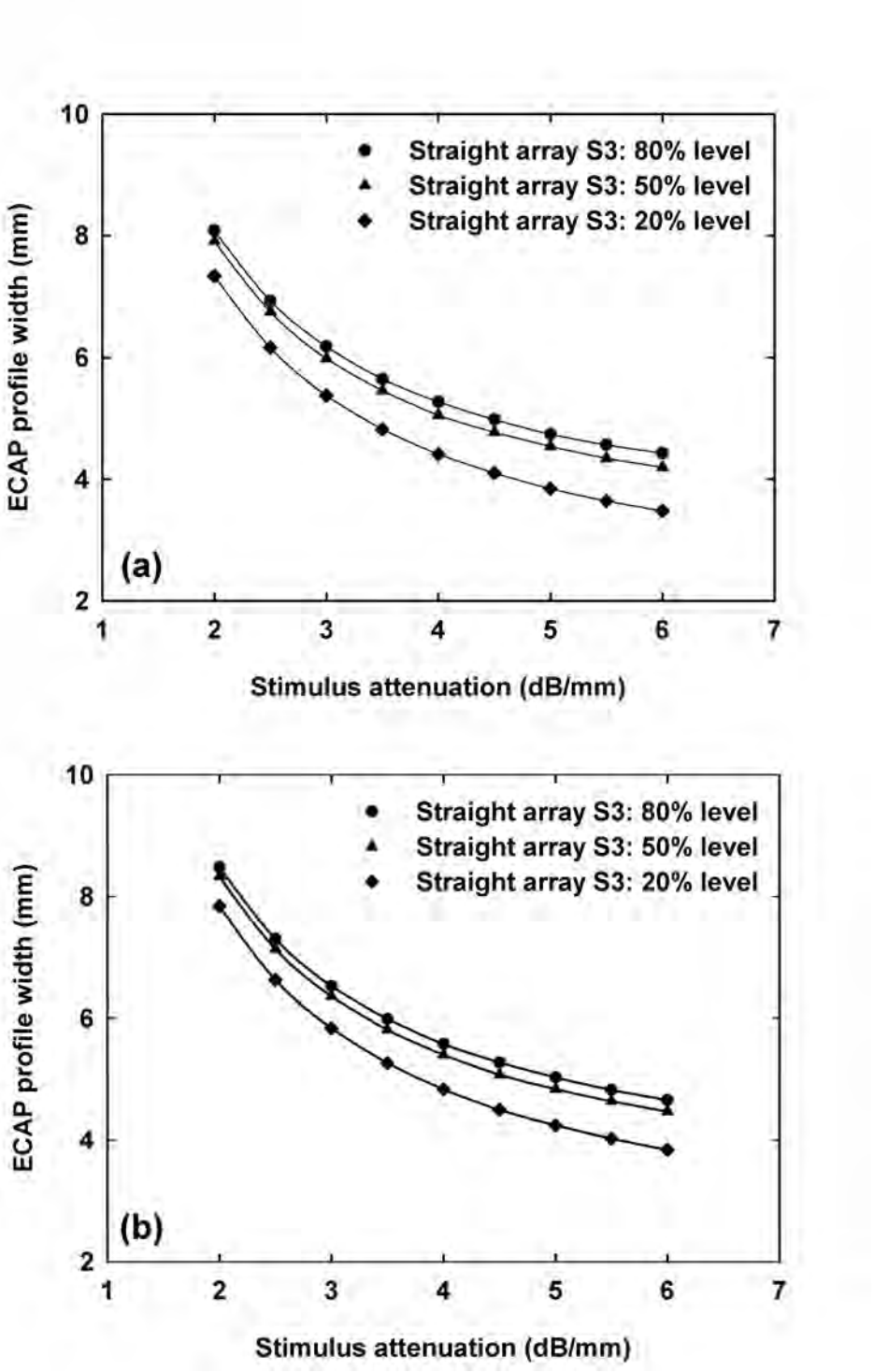

Figure 6.4: Predicted ECAP profile widths, at the electrode array level, for 20, 50 and 80% loudness levels for subject S3 (straight array) for (a) a degenerate and (b) a non-degenerate ANF population. The ECAP profile widths are plotted against stimulus attenuation.

Table 6.3: Stimulus attenuation values that provide the best fit of the modelled human ANF model data to the data of Cohen *et al.* (2003).

	80% loudness level	**50% loudness level**	**20% loudness level**
Straight array: degenerate	2.5 - 6.0 dB/mm	2.5 - 6.0 dB/mm	5.5 - 6.0 dB/mm
Contour array: degenerate	5.5 - 6.0 dB/mm	5.0 - 6.0 dB/mm	No data to compare with
Straight array: non-degenerate	2.5 - 6.0 dB/mm	2.5 - 6.0 dB/mm	4.0 - 4.5 dB/mm
Contour array: non-degenerate	5.5 - 6.0 dB/mm	5.0 - 6.0 dB/mm	No data to compare with

6.4 DISCUSSION

The modelled results for the human ANF model showed that, as the loudness levels (or stimulus intensity) increased, the ECAP profile width (i.e. neural excitation spread) increased. This agrees with the findings of Cohen *et al.* (2003) and Briaire and Frijns (2005). A comparison between the simulation results for the non-degenerate and degenerate nerve fibres showed more localised excitation spread for the contour array compared to the straight array. This is consistent with the observation that the straight array is located further away from the modiolus than the contour array, with a resultant wider potential field distribution, which causes a larger number of nerve fibres to be excited at a specific stimulus intensity relative to the threshold stimulus intensity, (e.g. Shepherd *et al.*, 1993; Cohen, Saunders and Clark, 2001; Frijns *et al.*, 2001; Cohen *et al.*, 2003).

The simulated neural response profile width data were sensitive to the value of the stimulus attenuation parameter chosen (see Figure 6.4 and Table 6.3). Larger parameter values predicted smaller spread of neural excitation. Also, a homogeneous, isotropic medium was assumed in the space between the neural and electrode array levels in the simple approximation method. This assumption is in contrast to an actual cochlea, where the conductivities of the different cochlear tissues vary significantly (see for example Frijns *et al.*, 1995). Since stimulus attenuation is a function of conductivity, predictions of neural excitation spread will be influenced by a non-homogeneous, anisotropic model of the space between the nerve fibres and the electrode array.

The observation that stimulus attenuation seemed to vary with stimulus intensity (Table 6.3) might be related to a more localised spread of excitation at lower stimulus intensities relative to that at higher stimulus intensities. Stimulus decay occurs in two directions: transversal (i.e. perpendicular to the electrode array) and longitudinal (i.e. in a direction parallel to the electrode array) because currents distribute in both directions throughout the cochlear tissue, as reported by Kral *et al.* (1998). It is possible that the weight that stimulus decay in each direction carries toward the determination of the neural excitation profiles is dependent on stimulus intensity. However, this hypothesis requires further investigation. Variations in cochlear structure and location of the electrode array inside the scala tympani could also lead to variations in the conductivity profile of the cochlear tissue between the array and the nerve fibres and could thus be responsible for observed intersubject variability in stimulus attenuation. A further observation is that the electrode-electrolyte interface impedance is a function of stimulus intensity (i.e., current density through the interface) (Ragheb and Geddes, 1990). The impedance of the electrode-electrolyte interface is disregarded in the volume-conduction model. In the model a current source is modelled instead of a potential source and the input current will be constant as long as the impedance of the electrode-electrolyte interface stays within required compliance limits. Hence the forward calculation problem does not dependent on the impedance. However, the data from Cohen *et al.* (2003), which are an integral part of the reverse calculation, include the effect of the interface impedance. Hence, the dependency of stimulus attenuation on stimulus intensity may partly be explained by the volume-conduction cochlear model characteristics, rather than the ANF model. Since the development of the volume-conduction model falls outside the scope of this study, these issues will be addressed in a follow-up study.

There was a marked difference in the stimulus attenuation parameter values between the GSEF and human ANF models that best predicted the experimental results. The value of 3.5 dB/mm predicted with the GSEF model was closer to the measured values of 0.54 – 1.09 dB/mm for monopolar stimulation in living cats performed by Black and Clark (1980) and Black *et al.* (1983), than the value of 5.5 dB/mm predicted with the human ANF model. However, the differences in cochlear structural morphology between animals and humans, differences in the number and percentage myelination of ANFs and innervation patterns of both inner and outer hair cells across species, may be physiologically significant and care must be taken when extrapolating the animal results to predict results in human implantees (Nadol Jr, 1988; Frijns *et al.*,

2001). Matsuoka *et al.* (2000b) also discussed the differences and similarities between animal and human data. In most animal studies, acutely deafened animals are used. Therefore, a larger relatively intact nerve fibre population is expected, in contrast to the more degenerative nerve fibre population of the longer-term deafened animal or human. Acutely deafened animal models can thus only give a best case scenario for the electrical excitation of the human ANF (Abbas and Miller, 2004). In many of the animal experiments, a single electrode is placed inside the cochlea (Van den Honert and Stypulkowski, 1984), while in humans multiple-electrode arrays are used. The anatomy of the animal and human nerve fibres also differs (Rattay *et al.*, 2001b; Briaire and Frijns, 2005). Thus, nerve fibre models based on animal physiology at this stage can only roughly approximate human ANF behaviour.

In general, ECAP profile widths calculated with the GSEF model (Figures 6.3(c) and (d)) were narrower than those calculated with the human ANF model (Figure 6.3(a) and (b)). Similar to the ANF model, the ECAP profile widths for both the straight and contour arrays decreased with a decrease in loudness level. The inclusion of non-homogeneous, anisotropic material properties in the inverse calculation of the ECAP profile widths could also improve the estimated value of the stimulus attenuation parameter and could relate this parameter to the specific location of the electrode array relative to the target nerve fibres. Individualised volume-conduction models that take the location of the electrode array relative to the target nerve fibres of a subject into account, could also improve the stimulus attenuation value estimate.

In spite of a number of shortcomings in the current model as discussed above, results suggested that matching predicted neural excitation profile widths to ECAP data by manipulation of the stimulus attenuation parameter could provide estimates of stimulus attenuation for specific subjects. An accurate estimate of stimulus attenuation could be useful in models that depend on stimulus attenuation to calculate excitation profiles (e.g. Bruce *et al.*, 1999c; Conning, 2006).

6.5 CONCLUSION

The human ANF model correctly predicts an increase in excitation spread with an increase in loudness level, as well as wider ECAP profile widths for the straight array

compared to those for the contour array. The model also predicted realistic ECAP profile width ranges for the straight array while the lower limit for the width ranges predicted for the contour electrode is comparable to measured width ranges.

It is observed that the fitting of modelled excitation profile widths to measured ECAP profile widths requires different stimulus attenuation values at different stimulation levels. Whether this actually indicates a shortcoming in the model is not certain since the impedance, which is related to stimulus attenuation, could be dependent on stimulus intensity. This observation thus suggests that the effects of stimulus intensity on the mechanisms of stimulus decay and on the electrode-electrolyte interface impedance require further investigation.